Processing Characteristics and Structure Development in Solid-State Extrusion of Bacterial Copolyesters: Poly(3-hydroxybutyrate-*co*-3-hydroxyvalerate)

Y. D. WANG, T. YAMAMOTO,* and M. CAKMAK†

Institute of Polymer Engineering, College of Polymer Science and Polymer Engineering, University of Akron, Akron, Ohio 44325-0301

SYNOPSIS

The bacterial copolyesters poly(3-hydroxybutyrate-*co*-3-hydroxyvalerate) have been successfully commercialized by ICI and are currently being distributed worldwide. Because of their bacterial origin, they are completely biodegradable. This has opened up numerous opportunities to develop new environmentally friendly products. The solid-state extrusion of a series of biodegradable copolyesters (P(3HB-3HV)) was performed in our laboratory with the aim of gaining fundamental understanding about their processability below their melting temperatures. The extrudability windows were found to span the temperature range from 135 to 150°C, depending on the composition of the samples under our experimental setup. The solid-state extrudates were found to exhibit an extra melting endotherm about 15–20°C above their normal melting temperature. This high temperature melting peak increasingly became dominant at lower extrusion temperatures. Wide angle X-ray diffraction studies did not indicate any phase change that might be responsible for this increase in the melting point. Contrary to the expectations, the solid-state extruded samples did not show significant chain orientation along the extrusion direction. This might be a result of fracture of the mass in the barrel into smaller pieces and their randomization during the course of their passage through the die. When the extrusion temperature was raised closer to the melting temperature, the quality of the extrudates was improved, and this was reflected in improvement of their mechanical properties. © 1996 John Wiley & Sons, Inc.

INTRODUCTION

The discovery of the naturally occurring biodegradable polymers, such as poly(3-hydroxybutyrate) [P(3HB), or PHB] and their subsequent large-scale development, including its copolymers with hydroxyvalerate (HV) [P(3HB-3HV)], has opened up numerous opportunities to develop new environmentally friendly products ranging from fibers and films to molded parts. These polymers have recently been successfully commercialized by ICI and are currently being distributed worldwide. Because of their bacterial origin, they can be obtained in exceptionally pure form without any inclusions of additives and/or stabilizers.

These polymers and copolymers exhibit unique thermal and structural characteristics. The most important of these characteristics is the ability to incorporate one monomer into the crystal structure of another (polydimorphism). This allows the copolymers to attain degrees of crystallinity as high as 50–70%. The second characteristic of these copolymers is that the wide range of properties can be tailored in by choosing appropriate ratios of HB to HV in the copolymers. For instance, the increase of HV content reduces the melting point of the copolymer without sacrificing crystallizability. The previous studies on these bacterial copolyesters concentrated on the identification of their crystal

* Present address: Industrial Research Institute of Ishikawa, RO-1, Tomizu Machi, Kanazawa, 920-02, Japan.

† To whom correspondence should be addressed.

Journal of Applied Polymer Science, Vol. 61, 1957–1970 (1996)
 CCC 0021-8995/96/111957-14

structures,[1] chemical compositions by nuclear magnetic resonance (NMR)[2] and infrared spectroscopy,[3] and crystallization and thermal behaviors.[4]

The crystal structure of P(3HB) was investigated by Yokoichi et al.[1] They found that this polymer crystallizes into orthorhombic lattice structure. And being similar to polypropylene in its chemical structure, it also forms left-handed 2 : 1 helix. The addition of the bulkier HV monomer was found to expand the unit cell, particularly the a-axis. As a result of this expansion effect, the long period was found to increase slightly with the increase of the HV composition. If HB is added to P(3HV), the unit cell of P(3HV) is not significantly influenced since, in this case, the sterically smaller molecules are added to the already expanded unit cell of P(3HV). Melting point versus composition curves exhibit eutectic-like minimum around 30% of HV content, below which the P(3HB) crystalline form is observed; above this composition, slightly expanded P(3HV) form is observed. These results attest to the existence of polydimorphism in these copolymers.[6]

Crystallization behavior as a function of copolymer composition was extensively investigated by Mitomo et al.[7] and Bloembergen et al.[3] They found that, generally, the increase of HV content decreases the rate of crystallization and drops the ultimate crystallinity from 60–80% to 40–50%.[3] When P(3HB) is melt crystallized from the quiescent conditions, the maximum spherulitic growth rate was observed at about 80°C;[8] and at 17% HV content, this temperature decreases slightly to about 75°C.[9] Since the increase of HV content reduces the crystallizability of the copolymers, air or water quenching results in a relatively amorphous structure. Since the glass transition temperature of these polymers is below the room temperature, these amorphous copolyesters gradually crystallize in the room temperature. This characteristic is particularly important for the investigations involving nonisothermal processes, such as melt spinning, film casting, and injection molding, where the polymer experiences significant cooling rates during the course of solidification step. It was reported[6] that the addition of small amounts of boron nitride greatly enhances the crystallization rates in polymers and copolymers of HB and HV. This is highly desirable in processes where rapid crystallization of polymer is essential.

Thermal stability is important in melt processing operations involving a screw extruder, etc., where highly localized temperature variations can occur as a result of high shear effects particularly between the flight tip and the barrel surfaces. P(3HB) and its copolymers with HV are known to undergo thermal degradation on melting as evidenced by molecular weight measurements.[10–13] Marchessault et al.[6] reported that P(3HB) starts degrading at around 225°C in thermogravimetic analysis (TGA). This onset of degradation temperature increases with increasing HV content and reaches 244°C at 21% HV content. The difference between the onset of degradation (Tonset) and melting temperature (T_m) actually increases with the increase of HV content from 35°C at 0% HV to 119°C at 21% HV content. This indicates that the copolymers of HB and HV are much more thermally stable than the P(3HB) homopolymer. This, however, does not necessarily indicate shear cracking stability, which is important in extrusion processes.

Mechanical properties of unoriented isotropic polymers and copolymers of HB and HV was reported by Marchessault et al.[6] The Young's modulus of P(3HB) homopolymer is about 1.6 GPa; this value decreases to about 0.6 GPa at 20% HV content, indicating that the addition of HV greatly increases the flexibility of the copolymers. In addition, they reported that the addition of boron nitride as a nucleating agent greatly improves the mechanical properties. They attributed this improvement to the reduction of spherulite size by nucleating agents.

The research that has been performed on P(3HB) and P(3HB-3HV) in the past is generally fundamental in nature, concentrating mainly on the chemical (architecture) and physical (thermal behavior, crystallization from solution and melt under quiescent conditions, crystal structure determination, etc.) properties of these polymers. There are only a limited number of studies related to the effects of processing conditions on the development of structure and the resulting mechanical, optical, and degradation characteristics of the manufactured parts.[10]

In this paper, we present our experimental results on the solid-state extrusion of P(3HB-3HV), including thermal behavior, structure development, and mechanical properties.

EXPERIMENTAL

Material

The bacterial copolyesters, poly(3-hydroxybutyrate-*co*-3-hydroxyvalerate) [P(3HB-3HV)], whose chemical structure is shown in Figure 1, were supplied in powder and pellet forms by ICI. The compositions of

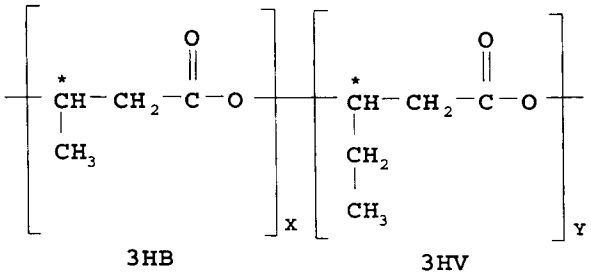

Figure 1 Chemical structure of P(3HB-3HV).

these materials used in this experimental study are listed in Table I.

As received, P(3HB-3HV) materials were vacuum-dried at 60°C for at least 48 h to remove the moisture. The dried powders and pellets were then subjected to the solid-state extrusion process immediately after drying.

Solid-state Extrusion Process

Solid-state extrusion was performed using a tabletop Instron capillary rheometer with a 5000 lbf (22240 N) compression load cell. The barrel diameter was 0.9525 cm. As shown in Figure 2, two special extrusion dies were designed and built in our laboratories. The dies were mounted on the Instron capillary rheometer with a special adapter. Since no continuous extrudate could be obtained with the large diameter die, the small diameter capillary die was used for all extrusion experiments.

First, the pellet or powder material was precompacted at 140°C with a force of 2000 lbf (8896 N), while the exit of the die was plugged. Since the melt viscosity of these materials are very low, this lower compacting temperature was necessary to remove the entrapped bubbles between the particulates. After the compaction, the barrel was heated to a preset temperature in 5–6 min. The preset temperature was 160°C for the pelletized materials and 170°C for the powdered material. The pressure was maintained on the compacted mass during the heating process. The compacted material was kept at the preset temperature for 10 min to achieve thermal equilibrium and for complete melting of the material. During the heating and equilibration stages, a slight temperature overshoot of about 6–7°C over the preset temperature was observed.

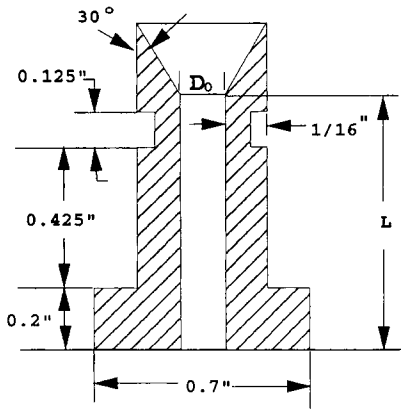

Die #	diameter (Do)	L	Area reduction ratio
1	3.34 mm	20.3 mm	8.13
2	1.41 mm	20.3 mm	45.63

Figure 2 Solid-state extrusion capillary geometry and dimensions.

To start the extrusion process, the barrel was first cooled to 155°C. The material was kept at this temperature for 15 min. The die plug was then removed, and extrusion was initiated with selected crosshead speed. After a sufficient amount of extrudates was collected for two different crosshead speeds, (XHS = 0.762, 7.62 mm/min), the extrusion was stopped, and the barrel was then cooled to the next temperature. These procedures were repeated at 5°C intervals until the lowest extrusion temperature was reached. The limit for this temperature was set by the load cell capacity. In addition, at temperatures

Table I Compositions of P(3HB-3HV) Samples Used in Study

Sample	Form	HV Content (wt %)	BN Content (wt %) Nucleating Agent	Triacetin Plasticizer (%)
1	Pellet	10.8	0.9	9.0
2	Powder	11.9	1.0	0.0
3	Pellet	4.5	0.9	9.0

below 130°C, the extrudates showed fragmented surface features, and they were quite easily broken. During the extrusion process, the extrusion force was recorded on a chart recorder. The force at steady extrusion was read off the chart when the force remained constant. Therefore, the force values presented in this paper represent uncorrected data. Such factors as pressure losses in the barrel and entrance correction were assumed to be uniform throughout the experiments.

Compression Molding Process

To study the thermal and crystallization behavior of these materials without the influence of solid state deformation, a film of Sample 1 was prepared at 170°C by the compression molding process. The dried pellets of Sample 1 were placed in a compression press. After the temperature equilibration for 3 min, the material was pressed under a 10 ton force for 3 min. The film sample was subsequently cooled to room temperature before it was removed from the mold. The film obtained was about 0.1 mm thick and was found to be void free.

Scanning Electron Microscopy (SEM)

The side surfaces of the selected solid state extrudates were examined using a Hitachi S-510 scanning electron microscope.

Thermal Characterization

Differential scanning calorimetry (DSC) thermal analysis of the extrudates and compression molded samples were performed using a DuPont DSC 910 apparatus. The samples of approximately 10 mg were crimped in the aluminum DSC pans and were scanned from room temperature up to a temperature where melting has completely finished with 20°C/min heating rate in a dry nitrogen atmosphere. The DSC analysis were also performed on the samples cut from the center regions of the materials left in the barrel after solid state extrusion process. The cutting procedure is shown in Figure 3.

Mechanical Properties

Tensile tests of the extrudates were performed on a Monsanto Tensometer (Model T-10) at room temperature. A gauge length of 2.5 cm and a 100%/min strain rate was used for all samples. The results obtained were averaged over three to five samples for each condition.

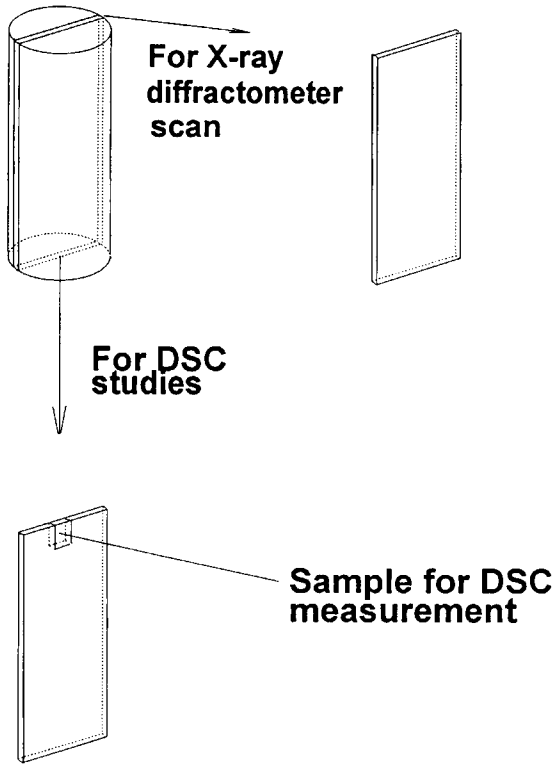

Figure 3 Sample cutting procedures for DSC and WAXRD studies.

Density Measurements

The density measurements were performed using a density column at 25°C. The extruded samples were immersed in the NaBr–water solution for two days before the measurements. The crystallinity was calculated from the density for each sample using the crystalline density ρ_c = 1.260 g/cm^3 and the amorphous density ρ_a = 1.177 g/cm^3.[14]

Hot Stage Video Microscopy

To identify the multiple endothermic peaks observed in the DSC scans, a Mettler hot stage (FP 84 HT) was used to monitor the melting sequence of the mass (sample 1) left in the barrel after the lowest processing temperature experiment was completed. The specimen for this experiment was prepared by slicing a 30 μm specimen in the direction normal to the symmetry axis of the cylindrical mass taken out from the barrel. The hot stage was placed on an optical microscope (Leitz Laborlux 12 POL S). The

heating scan was performed from 30 to 200°C at a heating rate of 20°C/min. The whole melting sequence was recorded on a video cassette through which the optical images at different temperatures were later captured and converted to 8-bit gray scale images using an image analysis system. The transmitted light intensity averaged over a large cross sectional area at each temperature was then obtained through an image analysis software. Since the experiment was performed under cross polarized light condition, the transmitted light intensity is depolarized light intensity and roughly proportional to the crystallinity of the sample. By tracing the transmitted light intensity as a function of temperature, one can monitor the crystallization and melting sequences that takes place at different temperatures.

Wide Angle X-ray Diffraction (WAXRD)

To evaluate the effect of the extrusion temperature on the average orientation development and the crystal structure, the extrudates obtained at different temperatures for Sample 1 were analyzed using a matrixing microbeam camera equipped with a precision x-y translation stage. This camera was mounted on a 12 kW Rigaku rotating anode generator, and a nickel foil filter was used to obtain CuK_α radiation. The X-ray beam size was 100 μm. The machine was operated at 40 kV and 150 mA. In this series of experiments, the whole extrudate was mounted on the sample holder, and the X-ray beam was focused on the cylindrical extrudate in such a way that it passed through the symmetry axis of the sample.

Wide angle X-ray scattering (WAXS) profiles were obtained on the compression molded sample, and the samples were cut from the cylindrical rods left in the barrel after the solid state extrusion process with the cutting procedure shown in Figure 3.

Small Angle X-ray Scattering (SAXS)

SAXS patterns were taken using a Rigaku RINT 1000 camera with nickel filtered CuK_α radiation. The exposure times were kept constant at 35 h, and the sample to film distance was 220 mm. The long periods of selected samples were calculated from their scattering patterns.

RESULTS

Solid-state Extrusion of P(3HB-3HV)

Before solid state extrusion was performed, the thermal properties of the as received samples were analyzed with DSC. As indicated in Figure 4, these copolyesters show a broad melting range starting well below 100°C and extending up to 170°C. They possess high levels of crystallinity, indicated by the absence of the cold crystallization peak and the high values of the heat of fusion. Based on these DSC spectra, we chose to do solid-state extrusion in 90–155°C range.

The extrusion process was first performed on Sample 1 using the larger die (Do = 3.34 mm). However, no continuous extrudates could be obtained in the 110–145°C temperature range. The extrudates obtained were in small pieces with sharp edges, indicating that the fracture of the larger mass in the barrel into small pieces has occurred at the entrance region of the capillary die. No or minimal cold deformation was observed using this die. This fracture behavior became more severe at lower processing temperatures, resulting in smaller broken pieces being discharged. At high extrusion temperatures (140 and 145°C), the quality of the extrudates was found to be improved, but it was not good enough for any practical application.

With smaller diameter capillary die (Do = 1.41 mm), better extrudates could be obtained in 135–

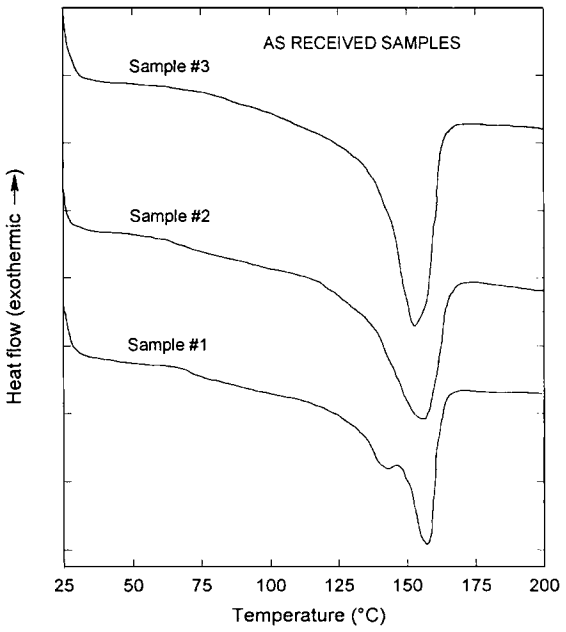

Figure 4 DSC thermograms on as-received samples.

150°C range. Therefore, smaller diameter capillary die was decided upon for the rest of this series of experiments.

Figure 5 shows the force at steady extrusion versus extrusion temperature obtained using the small capillary die (Do = 1.41 mm) for three different samples. As expected, higher crosshead speed results in higher force levels. As the extrusion temperature increases, the force at steady extrusion drops dramatically. At the temperatures near the melting peak temperature of the material, the force required to maintain steady extrusion becomes very low. Similar observations were also made by other investigators on PP[15] and VF2/VF3 copolymers.[16] As shown in Figure 6, the sample containing plasticizer (Sample 1) exhibits lower force at steady extrusion compared

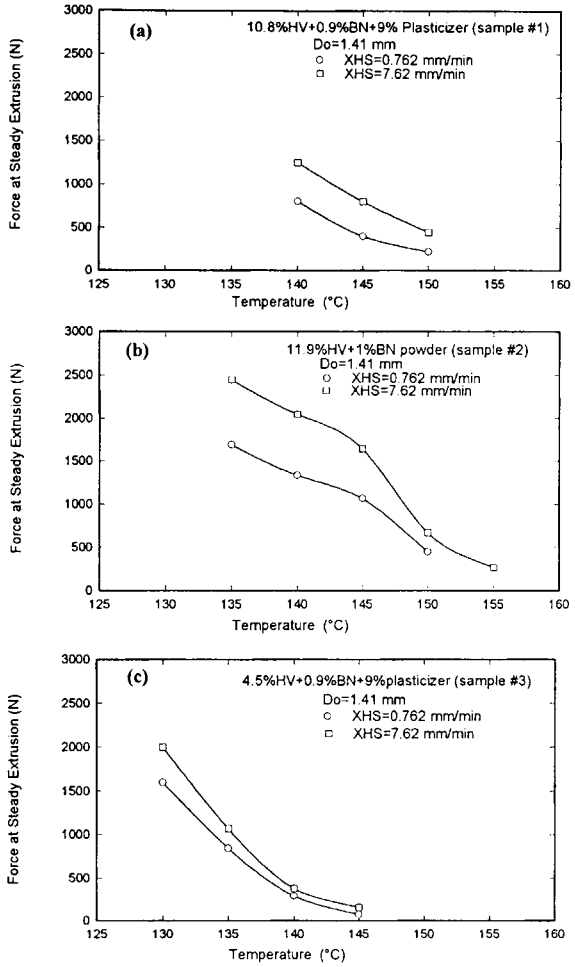

Figure 5 Force at steady extrusion vs. extrusion temperature for (a) P(3HB-3HV) Sample 1 at XHS = 0.762 and 7.62 mm/min, (b) P(3HB-3HV) Sample 2 at XHS = 0.762 and 7.62 mm/min, and (c) P(3HB-3HV) Sample 3 at XHS = 0.762 and 7.62 mm/min.

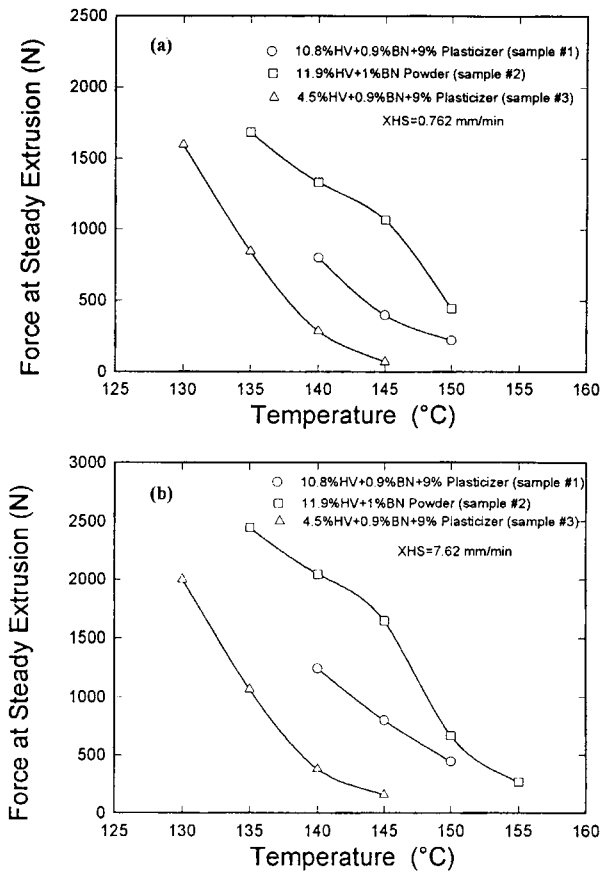

Figure 6 Force at steady extrusion vs. extrusion temperature for (a) XHS = 0.762 mm/min and (b) XHS = 7.62 mm/min.

to the sample containing no plasticizer (Sample 2) with roughly the same HV content. This figure also shows that the lower HV-containing copolymer (Sample 3) requires lower force for extrusion at the same processing temperature.

Based on the observation of quality of the extrudates under different processing conditions, the solid state extrudability windows for three different samples received are developed, and they are presented in Figure 7. This figure indicates that the inclusion of plasticizer helps open the processing window particularly at low extrusion speed. These processing windows are specific to the machine used in this experiment since the experiments were limited to the tolerance levels of the rheometer force transducer. With higher capacity machines, they are expected to expand towards the low temperatures. The filled circles represent the regions where high quality extrudates could be obtained, while the unfilled circles represent the extrudable regions with poor quality of the extrudates.

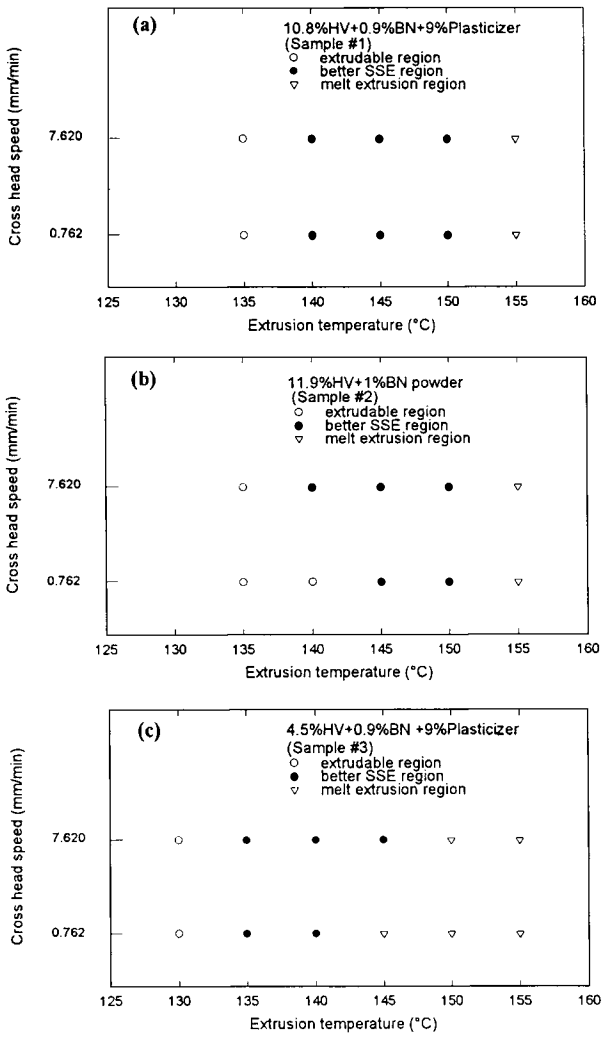

Figure 7 Solid-state extrudability window for all three polymers.

Figure 8 shows the surface qualities of selected extrudates at different temperatures. At the lower temperature side, the poor surface quality of the extrudates also accompanies poor mechanical performance. The solid state extrusion was not possible below 125°C due to the load cell limitation. At the higher temperature side represented by the unfilled triangles in Figure 7, the process is essentially a melt extrusion process. And due to very low melt viscosity exhibited by these sets of copolymers, the quality of the extrudates are controlled by the self drainage of the fluid mass from the barrel through the die. The extrudate quality could be improved by special cooling techniques (forced air, water trough, etc.), but this is beyond the scope of present paper.

As it can be observed in the Figure 7, the extrudability windows are situated above the melting start temperatures of the materials. With lower HV content (Sample 3), the extrudability window is slightly shifted to lower temperature. This can be better understood with the force at steady extrusion measurements. It was also found that higher crosshead speed (7.62 mm/min) results in better extrudates especially at lower extrusion temperatures. This may be as a result of improvement of interfragment diffusion by the increase of heat generated by the plastic deformation of the mass in the barrel. This also translates into higher mechanical properties.

Mechanical Properties

Tensile testing was performed only on the extrudates obtained at different temperatures at a extrusion cross head speed of 7.62 mm/min. The results are shown in Figure 9. The data are somewhat scattered. However, some trend can still be seen. The patterns of the modulus [Fig. 9(a)] and tensile stress at break [Fig. 9(b)] are very similar. As the extrusion temperature increases, the moduli tend to increase together with the tensile stresses at break. This is probably due to the improved thermal fusion of broken pieces at elevated temperatures, which leads to stronger extrudates. It is quite clear that the sample containing plasticizer (Sample 1) has lower moduli and tensile strength at break compared to the sample containing no plasticizer (Sample 2). The sample with lower HV content (Sample 3) possesses higher modulus and higher tensile strength than the sample with higher HV content (Sample 1). The results for the elongation to break are shown in Figure 9(c). As extrusion temperature decreases, the elongation to break increases. The higher the modulus and tensile strength, the lower the elongation to break. The sample containing plasticizer (Sample 1) has higher elongation to break than the sample containing no plasticizer (Sample 2) as expected.

Density Measurements

The density of each sample was measured using a density column in NaBr–water solution. The samples were immersed in the solution for two days before the measurements. The density data of the selected extrudates are tabulated in Table II. The crystallinity data calculated from the density data are plotted against extrusion temperature in Figure 10. In general, the density or the crystallinity of the

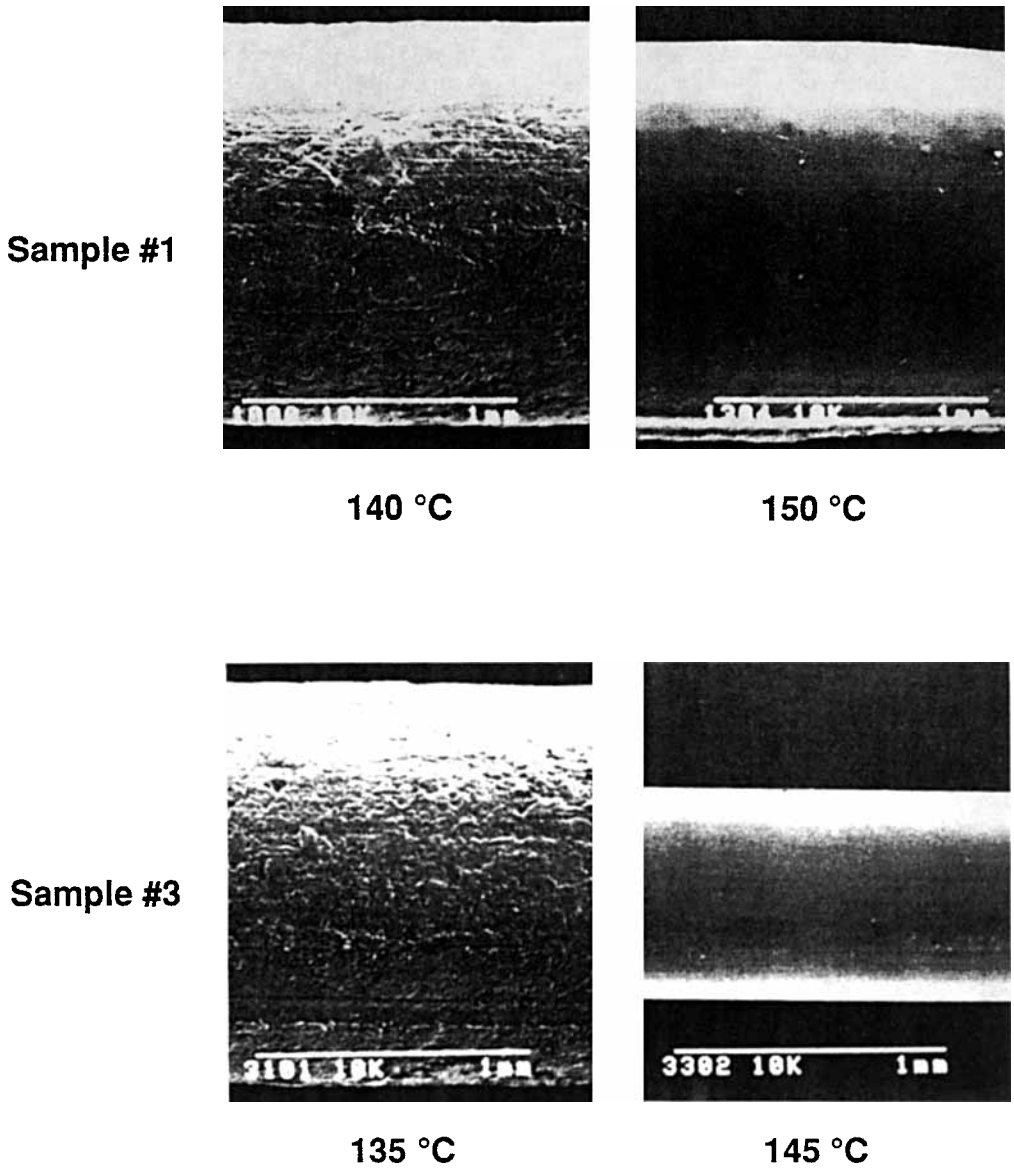

Figure 8 SEM surface photomicrographs of extrudates obtained at different extrusion temperatures.

extrudate depends on the composition of the sample. The lower the plasticizer content or the HV content is, the higher the density or the crystallinity of the extrudate becomes. The density increases very slightly as the extrusion temperature decreases.

Thermal Behavior of the Extrudates

Figure 11 show the thermal behavior of the extrudates obtained at different extrusion temperatures. With the exception of Sample 1 (10.8% HV + 0.9% BN + 0.9% Plasticizer), the DSC melting curves of the as-received pellets show one broad peak. When melted and cooled to the processing temperatures in the barrel and, subsequently, solid-state extruded, these polymers exhibit multiple endothermic peaks. As indicated in Figure 11(a), the sample extruded at 150°C show three distinct populations of melting peaks. One population melts around 140°C (population I), the second one melts about 160°C (population II), and the third one at about 170°C for plasticized copolymers and around 175°C for unplasticized copolymer.

The sample with 10.8% HV + 0.9% BN + 9% plasticizer behaves very similar to that without the plasticizer (11.9% HV + 1% BN). At 150°C pro-

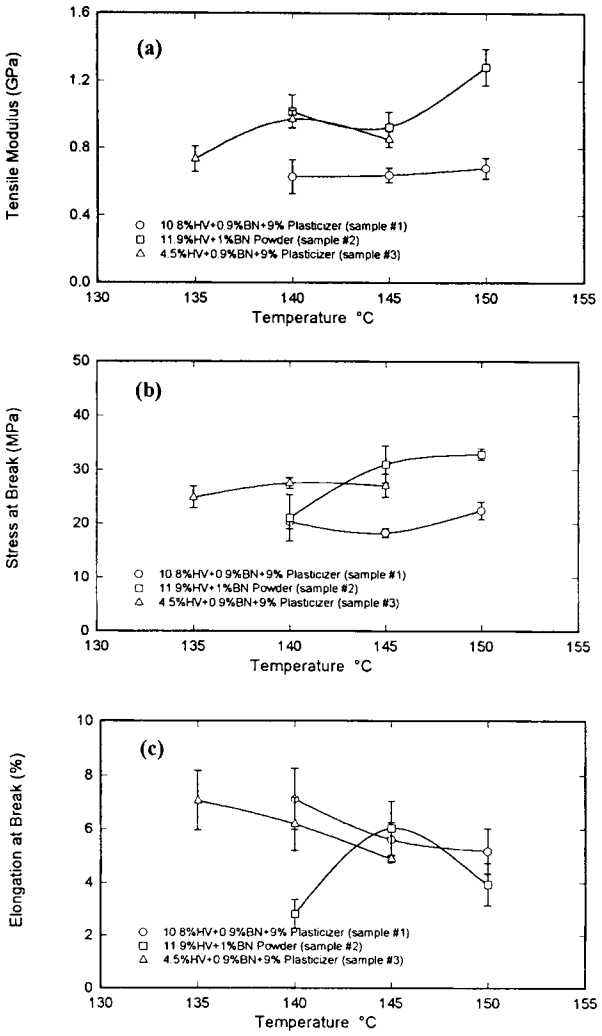

Figure 9 Mechanical properties vs. extrusion temperature for three different samples: (a) tensile modulus, (b) tensile strength at break, and (c) elongation at break.

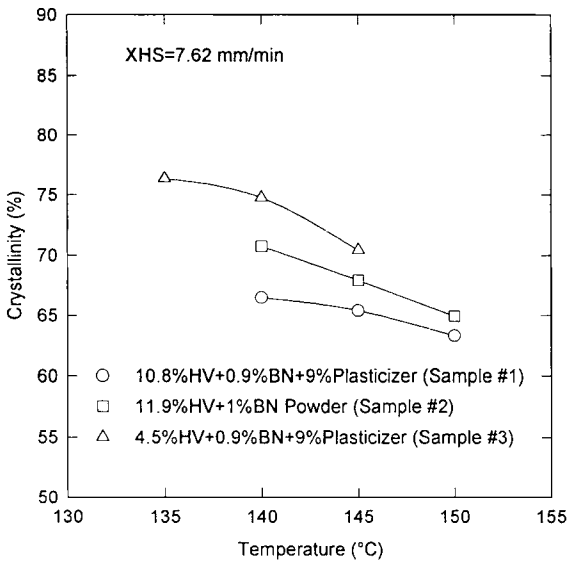

Figure 10 Crystallinity as a function of extrusion temperature for P(3HB-3HV) extrudates.

cessing temperature, the extrudates of these two samples exhibit three endothermic peaks. Population II, situated at 160°C, gradually disappears as the extrusion temperature decreases. Population III increases in size, and its peak becomes broader towards the lower temperature side. The area of the population I, on the other hand, slightly increases and its peak shifts towards lower temperatures. This behavior is very pronounced in Sample 3 (4.5% HV + 0.9% BN + 9% Plasticizer), where Population III is further developed with the reduction of population I, as we further decrease the extrusion temperature.

To investigate the origin or the condition leading to the formation of the Population III (high temperature), we examined the thermal behavior of the material left in (relatively) undeformed state inside the barrel after the lowest processing temperature experiments were completed. These DSC spectra are shown in Figure 12. These diagrams are very similar to those of extruded samples, indicating that the deformation caused by passage through the narrow die did not significantly affect the thermal behavior of these polymers.

It appears that Population I, whose peak position either remains constant or decreases, as in the case of samples 2 and 3, represents the lower melting,

Table II Density Data of Selected Extrudates

Sample	Density (g/cm³) at Extrusion Temperatures			
	135°C	140°C	145°C	150°C
1 (10.8% HV + 0.9% BN + 9.0% Plasticizer)		1.2309	1.2300	1.2282
2 (11.9% HV + 1.0% BN)		1.2346	1.2322	1.2296
3 (4.5% HV + 0.9% BN + 9.0% Plasticizer)	1.2394	1.2380	1.2343	

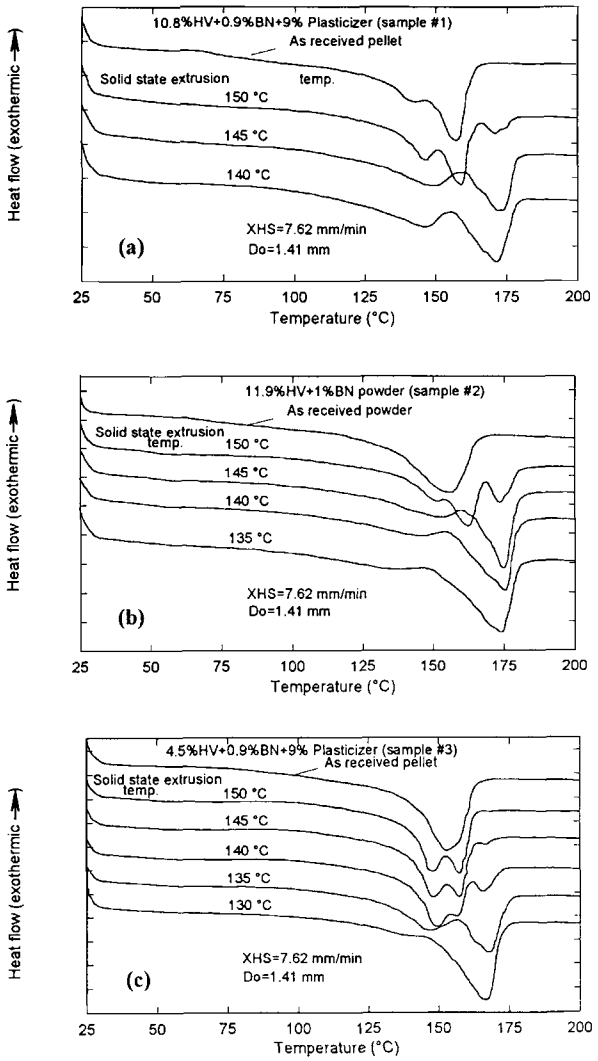

Figure 11 DSC thermograms of P(3HB-3HV) extrudates for (a) Sample 1, (b) Sample 2, and (c) Sample 3.

small, and/or disordered crystallite regions. This is evidenced by the increase of the breadth of this peak towards lower temperatures as the processing temperature is decreased.

To verify the origin of the higher melting peaks, a hot stage video microscopy experiment was performed under cross polarized light condition on the mass [same sample as sample 1 in Figure 12(a)] left in the barrel after the lowest processing temperature experiment was completed. As shown in Figure 12(b), the transmitted light intensity decreases slowly as the temperature increases up to 125°C, then it rapidly decreases in the temperature range from 125–150°C, indicating the melting of the crystals with lower melting temperature. In the range from 150–165°C, there appears a shoulder which slows down the speed of the intensity decrease. This small change in the slope of the intensity profile may indicate the existence of the recrystallization process during the heating process. As we further increase the temperature, the intensity decreases rapidly again due to the melting of the crystals with higher melting temperatures.

WAXRD Studies

WAXRD studies equatorial profiles of the samples cut from the cylindrical mass left in the barrel after solid state extrusion were obtained. As a reference, the profile of the compression molded sample was also taken. These WAXRD profiles are shown in Figure 13. The d-spacings calculated based on these profiles approximately match the results calculated based on the unit cell dimension reported by previous authors.[1,17] From these profiles, it can be seen that all these samples, including the compression molded sample, possess the same crystal structure

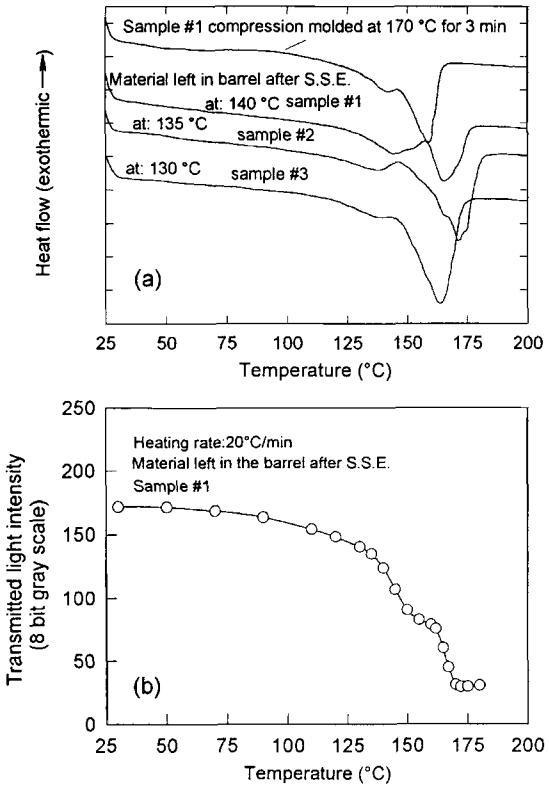

Figure 12 (a) DSC thermograms on samples that has undergone temperature–pressure cycle without deformation through the die (lowest processing temperatures). (b) Depolarized light intensity vs. temperature for Sample 1 in (a).

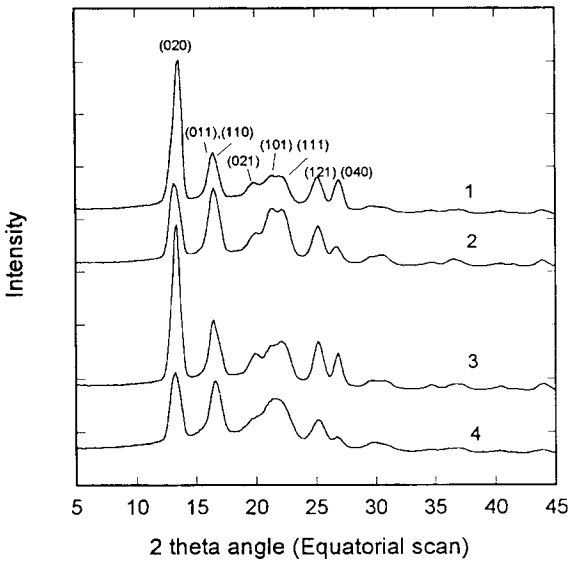

Equatorial scans:
1. mass left in barrel after SSE for sample #1
2. mass left in barrel after SSE for sample #2
3. mass left in barrel after SSE for sample #3
4. compression molded sample #1 (170 °C, 3 min)

Figure 13 WAXRD equatorial diffraction profiles of samples shown in Figure 12.

despite the fact that the samples removed from the barrel after solid state extrusion show a much higher melting temperature than the sample obtained by compression molding as indicated in Figure 12. Thus, it is clear that the appearance of this higher melting peak is not due to the change in crystal unit cell structure.

To study the orientation development during solid state extrusion, a series of WAXS pictures was taken on the extrudates of sample 1 obtained at different extrusion temperatures. In general, it is expected that the lower the extrusion temperature, the higher the molecular orientation level. However, it is not the case in solid state extruded P(3HB-3HV). As shown in Figure 14, all these extrudates possess almost random crystallographic orientation. This is a result of fracture of the mass in the barrel into smaller pieces and their randomization during the course of their passage through the die.

Small Angle X-ray Studies

Small angle X-ray scattering (SAXRS) patterns of selected samples are shown in Figure 15. The long spacing data calculated from these patterns are listed in Table III, together with the extrusion temperatures. The extrusion at lower temperatures causes the formation of diffuse halo without any variation in the azimuthal intensity profile. This indicates that the crystallites are not oriented and are rather aperiodic. As the extrusion temperature increases, the scattering halo becomes sharper and scattering intensity increases, indicating increased order in the structure is established at elevated temperatures. The long spacing also decreases very slightly with the decrease of the extrusion temperature. This general behavior is roughly the same for all compositions investigated. All the patterns show only one scattering ring indicating that the solid state extrudates possess only single distribution of crystallite size.

DISCUSSIONS

The increase of the melting temperature of some polymers after solid state extrusion process has also been observed by other investigators. Wang et al.[18] found very similar behavior on a polyimide (BTDA-

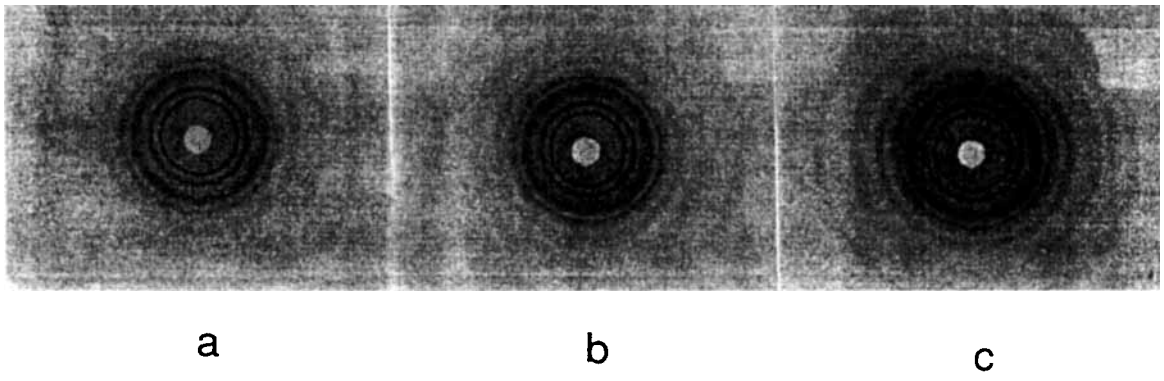

Figure 14 WAXRD film patterns on selected solid-state extruded samples.

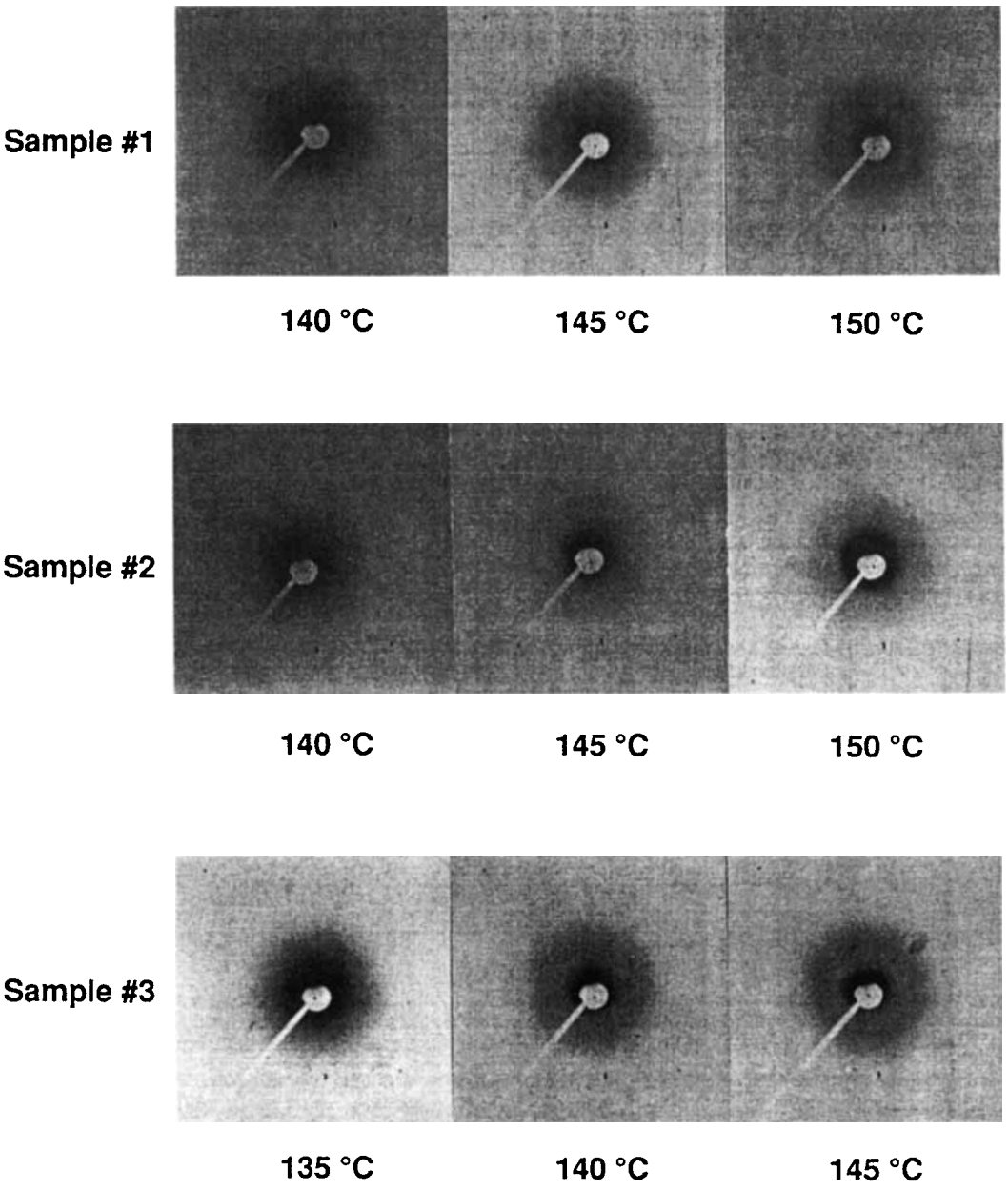

Figure 15 SAXRS film patterns on selected solid-state extruded samples.

DMDA) material. The existence of the higher melting peak in solid state extruded BTDA–DMDA samples was due to the melting of the crystals developed partially during the solid state extrusion process and partially during the recrystallization process at or above the lower melting temperature during the DSC scan as evidenced by DSC and hot stage video microscopy measurements. The recrystallized crystals exhibit several new peaks in their WAXS profiles, indicating the possible existence of a new crystalline transformation. Southern and Porter[19] also observed the same increases in melting temperatures of solid state extruded HDPE and attributed such observation to the extended chain structure. Lee and Cakmak[20] attributed the increases of the melting temperature of the solid state extruded VF_2/VF_3 copolymers to the crystallization under high compressive force before the actual extrusion. Weeks et al.[21] attributed the increase in the melting temperature of solid state extrudates to sig-

Table III Data Calculated from SAXRS Patterns of Selected Samples

Sample	Long Spacing (Å) at Extrusion Temperatures			
	135°C	140°C	145°C	150°C
1 (10.8% HV + 0.9% BN + 9% Plasticizer)		—	82	85
2 (11.9% HV + 1% BN)		70	72	74
3 (4.5% HV + 0.9% BN + 9% Plasticizer)	75	78	79	

nificant chain unfolding in the extrusion direction accompanied by lamellar thickening. On the other hand, Aharoni and Sibilia[22] attributed the increase to increased degree of crystalline perfection.

Multiple melting peaks in P(3HB-3HV) were also observed by other investigators. Mitomo and et al.[7,23] observed two melting peaks for the annealed P(3HB-3HV) samples with HV content ranging from 0–10 mol %. The solution-grown P(3HB) crystal showed two series of melting points at annealing temperatures below 150°C. The lower temperature series was found to increase linearly with the increase of annealing temperature, whereas the higher one was found to be essentially unchanged. With increasing heating rate, the higher melting peak shifted to the lower temperature and decreased in its area, whereas the lower melting peak remained unchanged. They then suggested that the lower temperature melting peak corresponds to the real melting point of the unannealed material, whereas the higher one is identified with the reorganized crystal during the heating process. Their SAXS studies proved that P(3HB) annealed at 145°C shows two long spacings, an original long spacing and a thicker one nearly corresponding to double of the original.[23] They concluded that the two series of melting peaks appeared at the lower and the higher temperatures correspond with two long spacings. The long spacing then increases hyperbolically as annealing temperature increases. Owen et al.[9] later observed the existence of double melting peaks of this copolymer and attributed the appearance of the higher melting peak to the reorganization of unstable crystals to more stable crystals during slow heating process. The two melting peaks have also been observed in the P(3HB-3HV) samples treated with methyl- and ethyl amines.[24]

In the solid state extrusion of P(3HB-3HV), as the extrusion temperature decreases, the positions of the higher melting peaks do not seem to change, and only the area under the higher melting peak increases while the area under the middle melting peak decreases. Our SAXS and transmitted light video microscopy studies support the idea that the existence of the higher melting peak is due to the melting of the higher melting crystals formed through the recrystallization process during the DSC heating scan.

CONCLUSIONS

It is possible to extrude P(3HB-3HV) copolyesters below their melting peak temperatures. The extrudability window is in the temperature range from 135–150°C under our experimental setup.

The P(3HB-3HV) samples obtained at lower processing temperatures generally show multiple endothermic peaks in their DSC scans. SAXRS and transmitted light video microscopy studies support the idea that the existence of the higher melting peak is due to the melting of the higher melting crystals formed through the recrystallization process during the DSC heating scan.

The solid state extruded samples did not show significant chain orientation along the extrusion direction. This is a result of fracture of the mass in the barrel into smaller pieces and their randomization during the course of their passage through the die. When the extrusion temperature is closer to the melting temperature, the quality of extrudates has improved, and this is reflected in improvement of their mechanical properties.

REFERENCES

1. M. Yokoichi, Y. Chatani, H. Tadokoro, K. Teranishi, and H. Tani, *Polymer*, **14**, 267 (1973).
2. H. Mitomo, T. Takizawa, and A. Keller, *Sen-i Gakkaishi*, **44**(7), 361 (1988).
3. S. Bloembergen, D. Holden, G. K. Hamer, T. L. Bluhm, and R. H. Marchessault, *Macromol.*, **19**, 2865 (1986).

4. M. Kunioka, A. Tamaki, and Y. Doi, *Macromol.*, **22,** 694 (1989).
5. T. L. Bluhm, G. K. Hamer, R. H. Marchesault, C. A. Fyfe, and R. P. Veregin, *Macromol.*, **19,** 2871 (1986).
6. R. H. Marchessault, T. L. Bluhm, Y. Deslandes, G. K. Hamer, W. J. Orts, P. R. Sundararajan, M. G. Taylor, S. Bloembergen, and D. A. Holden, *Makromol. Chem. Macromol. Symp.*, **19,** 235 (1988).
7. H. Mitomo, P. J. Barham, and A. Keller, *Polymer J.*, **19**(11), 1241 (1987).
8. P. J. Barham, A. Keller, E. L. Otun, and P. A. Holmes, *J. Mater. Sci.*, **19,** 2781 (1984).
9. A. J. Owen, J. Heinzel, Z. Skrbic, and V. Divjakovic, *Polymer,* **33,** 1563 (1992).
10. G. S. O'Brien, *Antec,* **39,** 2443 (1993).
11. N. Grassie, E. J. Murray, and P. A. Holmes, *Polym. Degrad. Stab.*, **6,** 47 (1984).
12. N. Grassie, E. J. Murray, and P. A. Holmes, *Polym. Degrad. Stab.*, **6,** 95 (1984).
13. P. J. Barham and A. Keller, *J. Polym. Sci.*, **24,** 69 (1986).
14. P. A. Holmes, *Development in Crystalline Polymers,* Vol. 2, edited D. C. Bassett, Ed., Elsevier, London, New York, 1988.
15. K. Nakamura, K. Imada, and M. Takayanagi, *Int. J. Polym. Mater.*, **2,** 71 (1972).
16. J. S. Lee and M. Cakmak, *Polym. Eng. Sci.*, **33,** 1559 (1993).
17. K. Okamura and R. H. Marchessault, *Conformational Aspects of Biopolymers*, Vol. 2, G. N. Ramachandran, Ed., Academic Press, London, New York, 1967.
18. Y. D. Wang, M. Cakmak, and F. W. Harris, *J. Appl. Polym. Sci.*, **56,** 837 (1995).
19. J. H. Southern and R. S. Porter, *J. Appl. Polym. Sci.*, **14,** 2305 (1970).
20. J. S. Lee and M. Cakmak, *Polym. Eng. Sci.*, **33,** 1570 (1993).
21. N. E. Weeks, S. Mori, and R. S. Porter, *J. Polym. Sci.*, **13,** 2031 (1975).
22. S. M. Aharoni and J. P. Sibilia, *J. Appl. Polym. Sci.*, **23,** 133 (1979).
23. H. Mitomo, P. J. Barham, and A. Keller, *Sen-i Gakkaishi,* **42**(11), 45 (1986).
24. H. Mitomo, *Sen-i Gakkaishi,* **48**(11), 595 (1992).

Received November 17, 1995
Accepted May 18, 1996